Acta Biochim Biophys Sin 2011, 43: 787–795 | © The Author 2011. Published by ABBS Editorial Office in association with Oxford University Press on behalf of the Institute of Biochemistry and Cell Biology, Shanghai Institutes for Biological Sciences, Chinese Academy of Sciences. DOI: 10.1093/abbs/gmr072.
Advance Access Publication 22 August 2011

Original Article

Monocyte chemoattractant protein-1 induces endothelial cell apoptosis *in vitro* through a p53-dependent mitochondrial pathway

Xuan Zhang, Xiping Liu, Huifeng Shang, Yan Xu, and Minzhang Qian*

Department of Biochemistry, Zunyi Medical College, Zunyi 563003, China
*Correspondence address. Tel: +86-852-8609792; E-mail: qian_mzh@hotmail.com

The cystine–cystine (CC) chemokine monocyte chemoattractant protein-1 (MCP-1) has been established playing a pathogenic role in the development of atherosclerosis due to its chemotactic ability of leading monocytes to locate to subendothelia. Recent studies have revealed more MCP-1 functions other than chemotaxis. Here we reported that various concentrations (0.1–100 ng/ml) of MCP-1 induced human umbilical vein endothelial cell (HUVEC) strain CRL-1730 apoptosis, caspase-9 activation, and a couple of mitochondrial alterations. Moreover, MCP-1 upregulated p53 expression of HUVECs and the p53-specific inhibitor pifithrin-α (PFTα) rescued the MCP-1-induced apoptosis of HUVECs. Furthermore, PKC (protein kinase C) activation or inhibition might also affect HUVECs apoptosis induced by MCP-1. These findings together demonstrate that MCP-1 exerts direct proapoptotic effects on HUVECs *in vitro* via a p53-dependent mitochondrial pathway.

Keywords MCP-1; endothelial cell; apoptosis

Received: February 27, 2011 Accepted: June 2, 2011

Introduction

Chemokines or chemotactic cytokines are a group of small (8–11 kDa) proteins that recruit circulating leukocytes to sites of inflammation or injury. Based on whether or not amino acid(s) inserted between the first two cysteine residues at N-terminal, chemokines were divided into the four subfamilies, CXC, CC, CX3C, and C [1]. They were considered mainly chemotactic, but recent studies revealed the versatilities of chemokines [2].

Monocyte chemoattractant protein-1 (MCP-1, CCL2) is the first identified CC subfamily member that can be secreted by many immune or non-immune cell types, including monocyte, endothelial cell (EC), smooth muscle cell, fibroblast, etc. MCP-1 plays a vital role in atherosclerosis by directing monocytes to permeate into the subendothelia where they become foam cells, and form fatty streak and finally atherosclerotic plaque [3]. Either MCP-1 or its receptor CCR2 deficiency reduced susceptibility to atherosclerosis [4,5]. Anti-atherosclerosis drugs might also work via MCP-1 repression in human ECs [6].

EC from all blood vessels maintained their anticoagulant properties [7], thus ECs apoptosis might lead to the pathogenesis of atherosclerosis [8]. Apoptotic ECs have been found in atherosclerotic lesions of both animal models and human patients. ECs in the lesions regenerated faster, showed increased pro-apoptotic proteins and decreased anti-apoptotic proteins [9]. Most atherosclerogenic risk factors were reported to evoke ECs apoptosis *in vitro* or increase circulating ECs *in vivo* [8], thereby disturbing vascular homeostasis, and increasing smooth muscle cell(s) proliferation, migration, and blood coagulation, which act as initiating events in atherogenesis [7,10]. It has been reported that *in vivo* local shear stress patterns or hyperglycemia influenced luminal EC apoptosis [11,12], and these factors determined atherosclerotic vulnerability and lesion size [13,14]. Therefore, the close relationship between ECs apoptosis and atherosclerosis has been acknowledged.

We have found that MCP-1 induced human umbilical endothelial vein cell (HUVEC) apoptosis characterized by cell proliferation inhibition, G_0/G_1 arrest, DNA fragmentation [15], upregulation of proapoptotic proteins Bax and Fas while downregulation of antiapoptotic protein Bcl-2 [16]. AnnexinV/FITC- propidium iodide (PI) staining also confirmed MCP-1 induced HUVEC apoptosis in which CCR2 was involved. It was found that MCP-1 induced CCR2 expression; either CCR2 antisense oligodeoxynucleotide or its antagonist inhibited MCP-1-induced HUVEC apoptosis *in vitro* [17]. These results indicated that MCP-1 not only promoted foam cell formation, but also induced EC apoptosis. However, the elaborate mechanisms of MCP-1-induced ECs apoptosis largely remain to be elucidated. In this paper, we reported the mechanisms of HUVECs apoptosis induced by MCP-1, through which we can better understand MCP-1 functions in ECs other

than chemotaxis and which will also enrich our knowledge about the relationship between chemokines and apoptosis.

Materials and Methods

Cell culture and growth curve

HUVEC strain CRL-1730 (ATCC) was cultured in complete DMEM/F12 culture medium (containing 20% FBS). HUVEC-specific marker von Willebrand factor (vWF) was detected with rabbit antibody (1:80 dilution; ZhongShan Golden Bridge, Beijing, China) by immunofluorescence.

Cultured cells were digested with 0.025% trypsin when grown into confluence, suspended with complete DMEM/F12 medium, stained with 0.04% trypan blue, and counted. Equivalent cells were inoculated in 24-well plates and cultured; cells in 3 wells were counted every 24 h for 8 days, then the cell growth curve was plotted.

MTT assay

Confluent cultured cells were digested with 0.025% trypsin and suspended with complete DMEM/F12 medium. Cells were counted and inoculated in 96-well plates at a density of 5×10^3 cells per well and cultured. After serum starvation with 1% FBS medium, synchronized cells were treated with MCP-1 (PeproTech, Rocky Hill, USA) at various concentrations (0.1–100 ng/ml) and further cultured for 48 h. Then, 20 μl MTT (5 mg/ml; Sigma–Aldrich, St Louis, USA) was added into each well and the resulting mixture was incubated for additional 4 h when violet crystals emerge. Supernatant was pipetted out and 100 μl DMSO was added into each well. The plates were oscillated for 10 min and scanned at 490 nm under a microplate reader (HumaReader, Human, Egypt).

Annexin V-FITC/PI double-staining flow cytometry

Synchronized cells were treated with MCP-1 and cultured for 48 h. Digested cells were collected by centrifugation at 1500 rpm for 5 min, washed with pre-cooled PBS (2000 rpm, 5 min) twice and resuspended with 250 μl binding buffer of Annexin V-FITC Apoptosis Detection Kit (KeyGEN Biotech, Nanjing, China). A total of 100 μl cell suspension was incubated with 5 μl Annexin V-FITC and 10 μl of 20 μg/ml PI for 30 min in the dark at room temperature and detected with a flowcytometer (Beckman Coulter, Fullerton, USA).

Detection of caspase-9 activity

Caspase-9 activity was measured using the caspase-9 assay kit (Beyotime, Haimen City, Jiangdu Province, China) with *N*-acetyl–Leu–Glu–His–Asp–P-nitroanilide (Ac-LEHD-*p*NA) as the colorimetric substrate as stated elsewhere [18]. Cultured HUVECs treated with various concentrations of MCP-1 for 48 h were washed, digested, and collected. A total of 100 μl cell lysates was obtained from 2×10^6 cells, incubated for 15 min on ice, then centrifuged at 16000 *g* for 10 min at 4°C. Protein concentration of the supernatants was measured with Bradford assay kit (Beyotime) and adjusted to 1–3 mg/ml. Each 10 μl supernatant was mixed with 10 μl Ac-LEHD-*p*NA (2 mM) in assay buffer. The 100 μl reaction mixture was incubated at 37°C for 2 h until absorbance at 405 nm was determined. The experiment was repeated three times and caspase-9 activity was expressed as fold(s) change over control (without colorimetric substrate) once corrected for baseline with *p*NA (10 mM).

Measurement of mitochondrial membrane potential ($\Delta\psi_m$)

MCP-1 pre-treated cells were incubated with 10 μg/ml fluorescent probe Rhodamine123 (Molecular Probes, Eugene, USA) at 37°C for 30 min as previously described [19] with minor modification. Cells were then washed in pre-cooled PBS (2000 rpm, 5 min) twice, and analyzed by flow cytometry with excitation wavelength 470–490 nm and emission wavelength 515–565 nm.

Determination of mitochondrial mass

Cultured HUVECs treated with various concentrations of MCP-1 were synchronized and collected as stated above. Mitochondrial mass was detected with NAO (10-*N*-nonyl acridine orange) staining cytometry [20]. Briefly, cells (1×10^6) were incubated with 100 nM NAO (Biotium, Hayward, USA) at 37°C in the dark for 15 min, and analyzed on a flow cytometer (FACS Calibur; Becton Dickinson, Mountain View, USA) with maximum absorbing wavelength of 519 nm and excitation wavelength of 495 nm.

Analysis of cytochrome *c* release

HUVECs were cultured, treated with various concentrations of MCP-1 for 48 h, synchronized and collected as stated above. Cells were suspended with PBS supplemented with 0.05% Triton-X 100 for 1 min, and washed with pre-cooled PBS twice; then blocked with goat serum (1:250 dilution; Boster BioTech., Wuhan, China) for 10 min. Mouse anti-human cytochrome *c* (cyt *c*) antibody (1:200 dilution; Santa Cruz Biotechnology, Santa Cruz, USA) was added and incubated at 4°C overnight. Cells were washed with pre-cooled PBS twice and treated with FITC-labeled goat anti-mouse IgG (1:200 dilution; ZhongShan Golden Bridge) at 37°C for 1 h. After washed with PBS, the cells were analyzed with flow cytometry.

Detection of intracellular calcium concentration $[Ca^{2+}]_i$

Intracellular Ca^{2+} concentration ($[Ca^{2+}]_i$) of HUVECs was measured by monitoring the fluorescence emission of Fura 2 using a spectrofluorophotometer (RF-1501; Shimadzu,

Kyoto, Japan) [21]. Cells were serum starved and synchronized, treated with various concentrations of MCP-1 (0.1–100 ng/ml) and 5 μM Fluo-3/AM. The mock control was treated only with 5 μM Fluo-3/AM. After 48 h of incubation, the flasks were gently oscillated for 45 min at 37°C and sit in room temperature for 15 min. Cells were then washed three times, centrifuged at 900 rpm for 5 min to exclude remaining Fura-2/AM outside membrane. Resuspended with Hanks buffer containing 0.2% BSA, HUVECs (2×10^6/ml) were transferred to quartz vials and detected by measuring 500 nm emission at 340/380 nm excitation. The cells were mingled with Hanks buffer containing 10% TritonX-100 to destruct the membranes (R_{max}), followed by perfusion with nominally Ca^{2+}-free Hanks buffer plus 500 mM EGTA to chelate Ca^{2+} (R_{min}).

The fluorescent emission was corrected for autofluorescence, and the 340/380 intensity ratio (R values) was recorded. $[Ca^{2+}]_i$ values were calculated using the formula: $[Ca^{2+}]_i = kDa\times(R-R_{min})/(R_{max}-R)$. The kDa value was taken as 224 nM.

Quantitative real-time reverse transcriptase-polymerase chain reaction

HUVECs were pre-treated with MCP-1 for 48 h, synchronized and washed with PBS. Total RNA from 10 cm^2 flasks was extracted with 1 ml RNAiso^{TM} plus reagent (TaKaRa, Osaka, Japan) according to the manufacturer's instructions. RNA concentration and integrity were determined with NanoDrop spectrophotometer and agarose gel electrophoresis.

Totally, 650 ng RNA was reverse transcribed into first-strand cDNA using PrimeScript RT reagent Kit (TaKaRa) in 20 μl reaction. Reverse transcription was performed as follows: 37°C for 15 min and 85°C for 5 s on Mastercycler (Eppendorf, Hamburg, Germany).

Then, 3 μl cDNA preparation was diluted to a final polymerase chain reaction (PCR) volume of 15 μl containing 7.5 μl SYBR Premix Ex Tag^{TM} II and 0.5 μl primers, and amplified with SYBR® PrimeScript® RT-PCR Kit II (TaKaRa) according to the manufacturer's instructions. PCR primers were: *p53* forward 5′-ACCACCATC CACTACAACTACAT-3′, *p53* reverse 5′-CAGGACAGG CACAAACACG-3′, *Actin* forward 5′-CCAGCCTTCCT TCTTGGGTAT-3′ and *Actin* reverse 5′-TTGGCATAGAG GTCTTTACGG-3′. Real-time PCR was performed under the following conditions: 95°C for 150 s; 40 cycles of 95°C for 10 s, 54.9°C for 20 s using Bio-Rad iCycler. The *p53* expression efficiency is calculated from the Ct values relative to that of *Actin*.

Western blot analysis

Cell lysates and supernatants of MCP-1 pre-treated or untreated HUVECs were obtained and the protein concentrations were determined as stated above. Protein samples (50 μg) were heated and then separated by 10% sodium dodecyl sulfate–polyacrylamide gel electrophoresis (SDS–PAGE). The proteins were transferred onto polyvinylidene fluoride membranes (Millipore, Bedford, USA), which were incubated with corresponding primary antibodies at 4°C overnight. The monoclonal antibodies against p53 and caspase-9 (1:200 dilution; Santa Cruz Biotechnology) were used, with β-actin (1:200 dilution; Beyotime) as an internal control. Washed membranes were incubated for 60 min with HRP-labeled goat anti-mouse IgG (Jackson ImmunoResearch, West Grove, USA). Membranes were washed again and subject to the BeyoECL Plus chemiluminescent kit (Beyotime) for chemiluminescence detection and then exposed to X-ray films.

Statistical analysis

Data analysis was performed using SPSS statistics software. Statistical significance was determined using the Student's two-tailed t-test. $P < 0.05$ was regarded as significant. All experiments were performed at least three times and the data were shown as mean ± SD.

Results

MCP-1-induced HUVECs apoptosis

HUVEC line CRL-1730 (ATCC) was cultured for 3–5 days until grown confluent. As shown under microscope, the majority of cells exhibited uniform and 'cobble stone' morphology [**Fig. 1(A)**]. Immunostaining the cells for EC specific marker vWF further confirmed that all cells were positive to anti-vWF antibody [**Fig. 1(B)**].

To analyze the effect of MCP-1 on HUVEC viability, MTT reduction assay was used to dye cultured HUVECs that were pre-treated with various concentrations of MCP-1 (0.1–100 ng/ml) for 48 h. **Fig. 1(C)** indicated that MCP-1 inhibited HUVECs proliferation dose dependently.

We further explored whether apoptosis took place in HUVECs when stimulated with MCP-1. MCP-1 pre-treated HUVECs were analyzed with PI- and FITC-labeled Annexin V double-staining flow cytometry. Annexin V bound specifically to phosphatidylserine (PS) exposed inside-out on the membrane, an early-phase apoptotic signal. Simultaneously, the dye PI was unable to pass through integrate cell membrane during the initial stages of apoptosis. MCP-1 increased early apoptotic HUVECs ($FITC^+/PI^-$) rate as compared with untreated control [**Fig. 1(D)**].

MCP-1 upregulated caspase-9 activity and expression

Caspase-9 is an important downstream molecule in the major apoptotic pathways. As shown in **Fig. 2(A),** caspase-9 activity increased dose dependently with MCP-1 as indicated by OD_{405} absorption with Ac-LEHD-*p*NA as the colorimetric

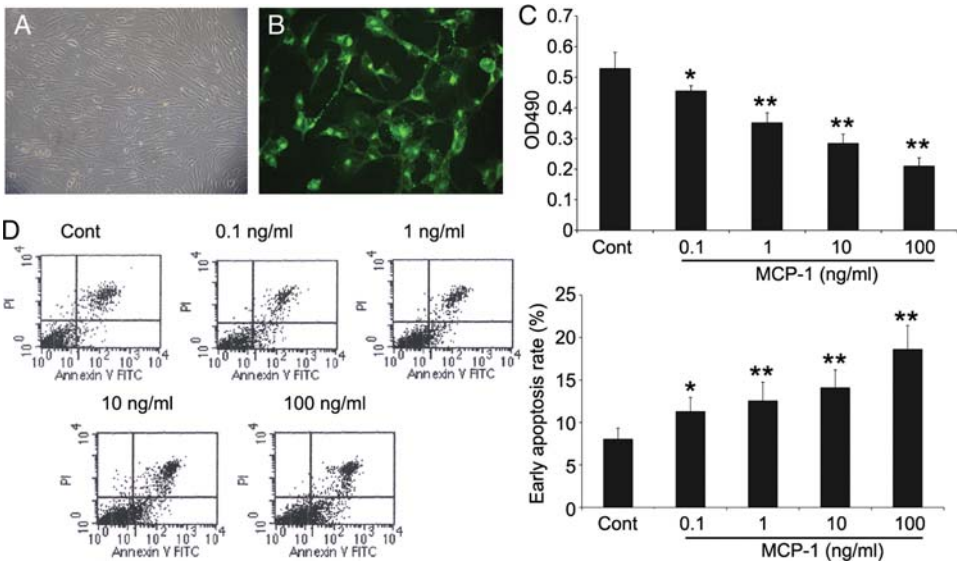

Figure 1 MCP-1 induced HUVECs apoptosis (A) HUVEC strain CRL-1730 (ATCC) was cultured in complete DMEM/F12 culture medium (containing 20% FBS) for 24 h. The cells appeared uniform ECs characteristic 'cobble stone' morphology. Original magnification 100×. (B) The cultured cells were immunofluorescent positive for EC-specific marker vWF. Original magnification 300×. (C) MTT assay indicated that MCP-1 inhibited HUVECs proliferation dose dependently. (D) After treatment with MCP-1(0.1–100 ng/ml) for 48 h, apoptosis rate was detected. MCP-1 increased HUVECs early apoptotic ($FITC^+/PI^-$) rates as compared with Cont. Cont, cells not treated with MCP-1. $^*P < 0.05$, $^{**}P < 0.01$ compared with the Cont. Data were expressed as mean ± SD from three separate experiments.

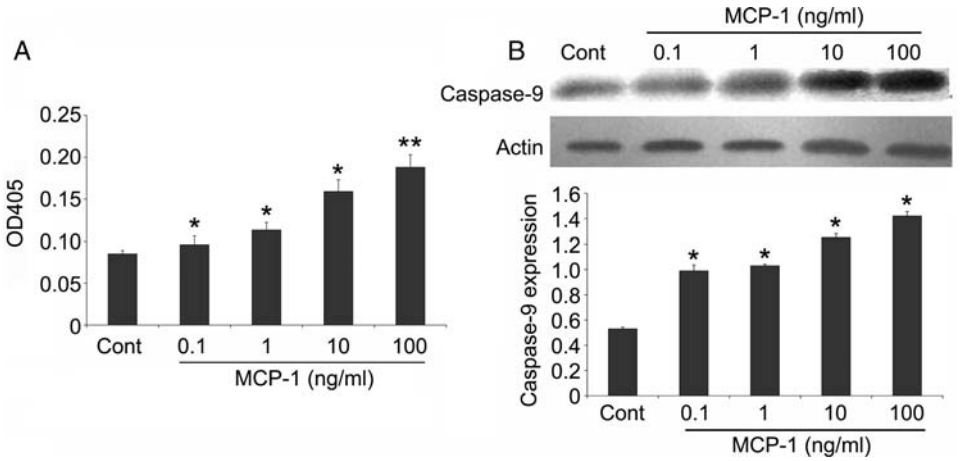

Figure 2 MCP-1 upregulated caspase-9 activity and expression (A) After treatment with MCP-1 (0.1–100 ng/ml) for 48 h, HUVECs lysates were subject to enzymatic assay with Ac-LEHD-*p*NA as the colorimetric substrate. Absorbance at 405 nm (OD405) was determined. (B) HUVECs caspase-9 expression was also upregulated in a similar trend as detected by western blot. Actin was used as a control. Cont, cells not treated with MCP-1. $^*P < 0.05$, $^{**}P < 0.01$ compared with the Cont. Data were expressed as mean ± SD from three separate experiments.

substrate. Meanwhile, caspase-9 expression of HUVECs was also upregulated by MCP-1 treatment in a similar trend [**Fig. 2(B)**] as detected by western blot. These findings demonstrate that MCP-1-induced caspase-9 activity at least partially is due to the increase of its protein expression.

Mitochondria were involved in MCP-1-induced HUVECs apoptosis

Caspase-9 is mainly considered as a mitochondrial apoptotic pathway involved signal. We thus turned our attention to mitochondrial perturbations of HUVECs after MCP-1 treatment.

The membrane-permeable cationic fluorescent dye Rh123 was used to determine the mitochondrial membrane potential of living cells. As to the same cell type, the volumes of mitochondria varied little; Rh123 fluorescence was proportionate almost exclusively to the absolute amount of the dye accumulated in mitochondria, hence the potential across mitochondrial membrane ($\Delta\Psi$). MCP-1 dose dependently reduced HUVECs mitochondrial membrane potential as implicated by decreased fluorescence detected by flow cytometry [**Fig. 3(A)**].

Next, we sought to determine mitochondrial mass. NAO (10-*N*-nonyl acridine orange) is a derivative of acridine

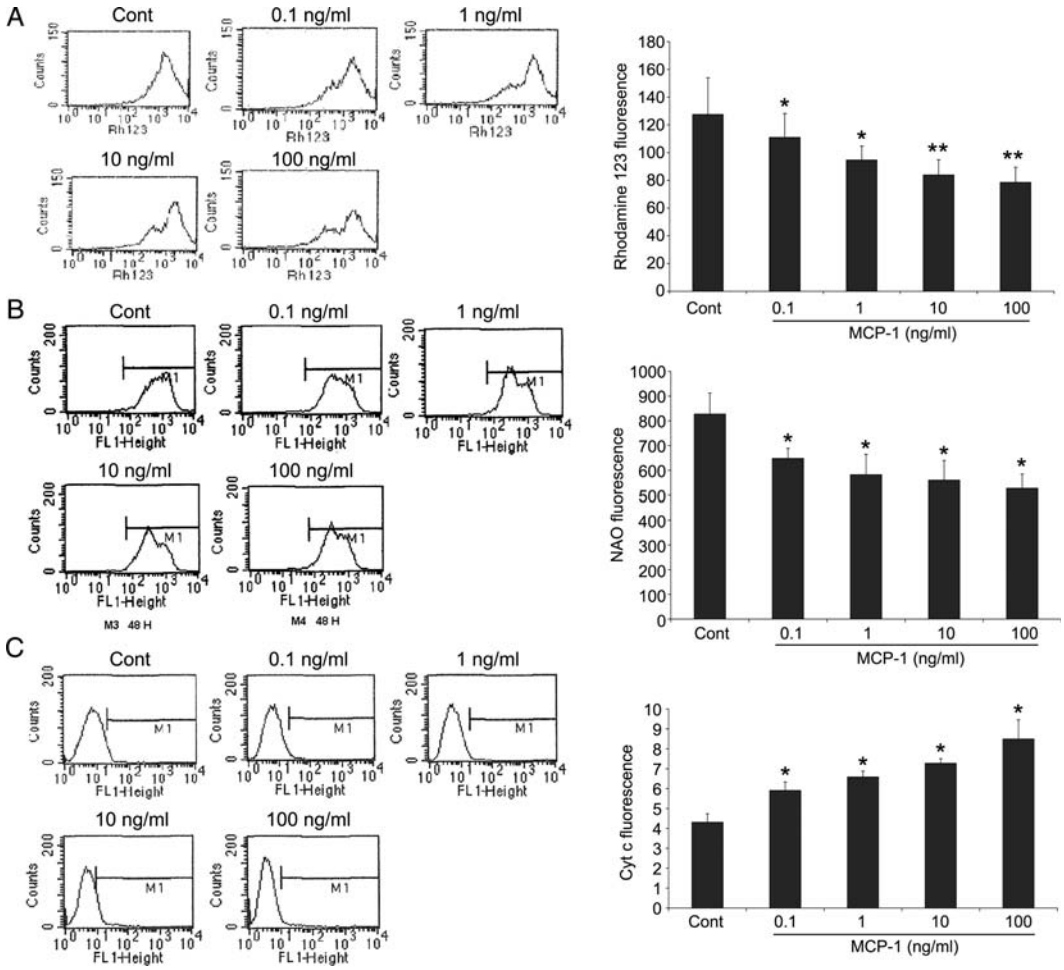

Figure 3 Mitochondria involvement in MCP-1-induced HUVECs apoptosis After HUVECs were treated with MCP-1 (0.1–100 ng/ml) for 48 h, indicators for mitochondrial membrane potential ($\Delta\psi_m$) and mitochondrial mass, and labeled cyt c antibody were separately loaded for following flow cytometry. (A) Rh123 fluorescence reduction indicated that HUVECs mitochondrial membrane potential was decreased by MCP-1 treatment. (B) NAO fluorescence reduction implied that MCP-1 treatment resulted in decrease of HUVECs mitochondrial mass. (C) Mitochondrial cyt c fluorescence decreased and meanwhile cytoplasmic cyt c fluorescence increased, indicating that MCP-1 promoted HUVECs cyt c release. Cont, cells not treated with MCP-1. $^*P < 0.05$, $^{**}P < 0.01$ compared with the Cont. Data were expressed as mean $\pm$ SD from three separate experiments.

orange, specifically binds to the negatively charged phospholipid cardiolipin on the inner membrane of mitochondria independent of the mitochondrial energy state. It is thus an appropriate marker of the mitochondrial membrane surface per unit of cell mass. After being stimulated with MCP-1 for 48 h, HUVECs mitochondrial mass decreased dose dependently [**Fig. 3(B)**].

An important event in mitochondrial apoptotic pathway is cyt *c* release. As shown in **Fig. 3(C)**, mitochondrial cyt c fluorescence decreased and meanwhile cytoplasmic cyt c fluorescence increased, indicating that MCP-1 treatment promoted HUVECs cyt c release.

p53 played an important role in MCP-1-induced HUVECs apoptosis

Since p53 transcription either dependently or independently activates genes in both extrinsic and intrinsic apoptotic pathways, we examined p53 expression of HUVECs treated with MCP-1 for 48 h. The mRNA level of *p53* was quantified by real-time PCR, and all samples were exactly amplified as indicated by amplification curves and melting curves (not shown). MCP-1 raised *p53* mRNA level of HUVECs [**Fig. 4(A)**]. Western blot also confirmed that MCP-1 enhanced p53 expression [**Fig. 4(B)**].

HUVECs pre-treated with MCP-1 (10 ng/ml) were pre-incubated with the various concentrations of the p53-selective inhibitor pifithrin-α (PFTα) for 30 min. As revealed by Annexin V-FITC/PI double-staining flow cytometry, 30 μM PFTα rescued EC apoptosis induced by MCP-1 [**Fig. 4(C)**].

Protein kinase C modulated MCP-1-induced HUVECs apoptosis

We investigated whether or not intracellular calcium perturbations happened during MCP-1-induced HUVECs apoptosis using the fluorescent indicator Fura-2 acetoxymethyl

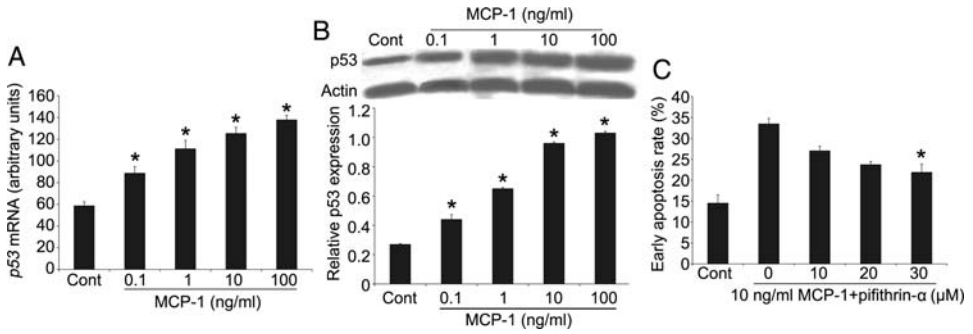

Figure 4 p53 played an important role in MCP-1-induced HUVECs apoptosis After treated with MCP-1 (0.1–100 ng/ml) for 48 h, p53 mRNA (A) and protein (B) levels were both found to be upregulated. Cont, cells not treated with MCP-1. $*P < 0.05$, $**P < 0.01$ compared with the Cont. (C) HUVECs were pretreated with pifithrin-α (10–30 μM) for 30 min and followed by 10 ng/ml MCP-1 treatment for 48 h. HUVECs apoptosis was only rescued by 30 μM pifithrin-α as revealed by Annexin V-FITC/PI double-staining flow cytometry. $*P < 0.05$ compared with cells treated with 10 ng/ml MCP-1 alone. Data were expressed as mean ± SD from three separate experiments.

ester (Fura2-AM). The ester form permeated membrane and was hydrolyzed by plasma esterases; free Fura2 combined with intracellular calcium. Quiescent HUVECs $[Ca^{2+}]_i$ was detected as 153.85 ± 4.94 nM, and MCP-1 stimulation augmented intracellular calcium concentrations $[Ca^{2+}]_i$ significantly [**Fig. 5(A)**].

After being treated with protein kinase C (PKC) activator phorbol 12-myristate 13-acetate (PMA) and PKC inhibitor chelerythrine, respectively, HUVECs were treated with 10 ng/ml MCP-1 and then the apoptosis rate was detected by flow cytometry. Different concentrations of PMA (0.1, 1 μM) enhanced cell apoptosis induced by MCP-1 ($P < 0.05$, $P < 0.01$) [**Fig. 5(B)**]. Chelerythrine (1 nM) treatment for 12 h impeded HUVECs apoptosis induced by MCP-1 ($P < 0.05$) [**Fig. 5(C)**].

Discussion

Atherosclerosis is a serious chronic cardiovascular disease that is influencing a large portion of the modern population. Chemokine MCP-1 is an assured risk factor [4,5]. Besides its conventional role of chemotaxis and proinflamation, we found that it was proapoptotic to HUVEC, which might be a new view for the roles of MCP-1 in the initiation and development of atherosclerosis. We believe that MCP-1 exerts far more complicated functions in atherosclerosis than our current knowledge. So, we investigated the mechanisms of this new function of MCP-1 to HUVEC.

At first, we verified MCP-1 induced HUVECs apoptosis *in vitro* by cytometry, and detected elevated caspase-9 expression and activity. It was reported that plasma MCP-1 level ranged from 0.1–0.4 ng/ml in patients of cardiovascular diseases [22,23]. An *in vitro* study also revealed that MCP-1 manifested monocytic chemoattractant activity at very low concentration and reached highest at 100 ng/ml [24]. To mimic the micro-environment that HUVEC experience *in vivo*, MCP-1 concentrations used in this study precisely cover its chemotactic and atherogenic ability.

Next, we checked whether the mitochondrial pathway was involved in apoptosis. The results showed that the structural and functional integrity of HUVECs mitochondria was challenged by MCP-1 treatment, including membrane potential and mitochondria mass decrease, cyt *c* release, etc. The roles of mitochondria in apoptosis are complex. Various proapoptotic stimuli were directly responsible for mitochondrial apoptotic events, including loss of mitochondrial transmembrane potential, release of cyt *c* or other apoptosis activators normally residing in the intermembrane space of mitochondria [25]. The mitochondrial masses reduced due to the destabilization process. The released molecules translocated to cytosol and/or nucleus, activated caspases, or hindered the actions of cytosolic antiapoptotic proteins [26]. The interactions between pro- and anti-apoptotic proteins and downstream effects led to cell cycle arrest and finally apoptosis.

In addition, the present study revealed the role of p53 in MCP-1-induced HUVECs apoptosis. p53 was upregulated by MCP-1 and the p53-specific inhibitor PFTα rescued the MCP-1-affected HUVECs apoptosis. p53-induced apoptosis was reported to be regulated by target gene transcription dependent and independent signaling pathways [27,28]. Mihara *et al.* reported that the p53 protein directly bound to the protective BclXL via its DNA binding domain and the Bcl2 proteins, unveiling the key to the mechanism of stress-induced apoptosis. The p53–BclXL–Bcl2 complexes induced permeabilization of the outer mitochondrial membrane, resulting in cyt *c* release [29]. PFTα is a reversible inhibitor of p53-mediated apoptosis and p53-dependent gene transcription. It has been reported that 30 μM PFTα prevents doxorubicin-induced HUVEC apoptosis [30], which is similar to the results of our study.

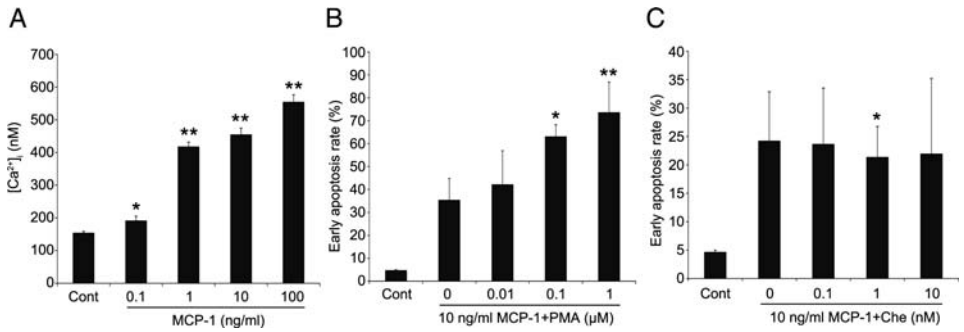

Figure 5 PKC modulated MCP-1-induced HUVECs apoptosis (A) MCP-1(10 ng/ml) stimulation for 48 h augmented intracellular calcium ($[Ca^{2+}]_i$) concentrations. Cont, cells not treated with MCP-1. $*P < 0.05$, $**P < 0.01$ compared with the Cont. After being treated with different concentrations of PKC activator PMA (0.01−1 μM) (B) or PKC inhibitor chelerythrine (0.1−10 nM) (C) for 12 h, HUVECs were induced by 10 ng/ml MCP-1 for 24 h, and then the apoptosis rates were detected by using FCM. Cont, cells not treated with MCP-1. $*P < 0.05$, $**P < 0.01$ compared with the cells treated with 10 ng/ml MCP-1 alone. Che, chelerythrine. Data were expressed as mean ± SD from three separate experiments.

PKC has been demonstrated both pro-apoptotic and anti-apoptotic in different cell types [31]. Ca^{2+} or diacylglycerol (DAG) binding might cause PKC conformational changes and increase its hydrophobicity, which facilitates its translocation and binding to plasma membrane [32]. Since PKC activation is Ca^{2+} dependent, we examined intracellular calcium concentration and found it was raised after MCP-1 treatment. The PKC activator PMA enhanced MCP-1-induced HUVECs apoptosis, which was attenuated by PKC inhibitor chelerythrine. As proved by other studies, MCP-1-induced HUVECs apoptosis was enhanced by 100 nM PKC activator PMA [33,34], but was impeded by 1 nM PKC inhibitor chelerythrine [35−37]. A previous study demonstrated that the IC_{50} value of chelerythrine to PKC is 0.7 μM [38]. While the concentrations we used rendered only partial inhibition of PKC, the early apoptosis induced by MCP-1 was partially rescued, and there might be an optimal concentration that worked nicely. Thus, PKC may also modulate MCP-1 induced HUVECs apoptosis.

The peripheral blood MCP-1 [22,23] can be both chemotactic [24] and proapoptotic [15,39]. The dual effect of MCP-1 on HUVEC may at least partially be explained by 'monocyte-endothelial cell interactions' [40]. The monolayer ECs contribute a lot to the integrity of endothelium where the apoptosis and turnover of ECs strike a balance under normal condition. When apoptotic rate of EC increases, for example, affected by MCP-1, such balance breaks and the precisely controlled permeability of intima increases. Sequentially, infiltration of monocytes and smooth muscle cells is increased, lipids are inhaled and deposited, plaques are formed, and ultimately the vasculature is damaged, such as atherosclerosis.

Recent studies showed that chemokines and their receptors were implicated in apoptosis. Hesselgesser *et al*. first discovered that human immunodeficiency virus (HIV-1) infected hNT neurons apoptosis when the virus envelope glycoprotein gp120 bound to its co-receptor CXCR4 instead of the other co-receptor CD4 [41]. Through the same chemokine receptor, gp120 induced CD8-positive T cells apoptosis [42]. The both effects could be verified by stromal-derived factor-1 (SDF-1), the physiological ligand of the chemokine receptor CXCR4 [41,42]. Chemokines are also revealed to be involved in apoptosis. The CXC chemokine CXCL12 (SDF-1α) produced by melanoma cells is capable of upregulating CCL5 production and initiating tumor-infiltrating lymphocytes (TIL) cell death [43]. Neutralization of the chemokine CXCL10 with its antibody reduced neuron apoptosis after spinal cord injury [44]. Chemokines not only induce neuronal and immunological cells, but also other sorts of cells, death. We reported here the chemokine MCP-1-induced vascular cell apoptosis. Thus, the mechanisms of apoptosis regulated by chemokines are complicated.

It was thought that the induction of epithelial cell apoptosis might counteract angiogenesis [45], and there indeed is some solid evidence [46,47]. MCP-1 has been recognized as an established direct angiogenic factor [48,49]. However, we demonstrated here that MCP-1 was proapoptotic to HUVECs *in vitro*. We proposed that maybe the cells themselves and the growth microenvironment account for the difference. We introduced the established HUVEC strain CRL-1730 (ATCC) in our study, while other investigators used primary cell isolated from neonatal umbilical cord that might be contaminated by other sorts of cells. Also the established cell strain may chance some biological changes beyond our recognition. Another possibility is that additives in the medium like vascular endothelial growth factor might contribute to angiogenesis by which MCP-1 apoptotic effect might be masked [49]. A novel zinc finger transcription factor MCP-1-induced protein (MCPIP) has been reported to act as a proapoptotic factor in other cell types when stimulated with MCP-1 [39,50]. We found that this protein was immediate early expressed in MCP-1-treated HUVECs (unpublished data), but how this factor

involves in MCP-1-induced apoptosis is expected to be figured out in future research.

In conclusion, our findings provide direct and clear evidence that MCP-1 facilitates HUVECs apoptosis *in vitro* via a p53-dependent mitochondrial pathway, which opens a new window for the vision of MCP-1 actions in the development of atherosclerosis.

Funding

This work was supported by a grant from the National Natural Science Foundation of China (30760078).

References

1 Allen SJ, Crown SE and Handel TM. Chemokine: receptor structure, interactions, and antagonism. Annu Rev Immunol 2007, 25: 787–820.
2 Charo IF and Ransohoff RM. The many roles of chemokines and chemokine receptors in inflammation. N Engl J Med 2006, 354: 610–621.
3 Niu J and Kolattukudy PE. Role of MCP-1 in cardiovascular disease: molecular mechanisms and clinical implications. Clin Sci (Lond) 2009, 117: 95–109.
4 Gosling J, Slaymaker S, Gu L, Tseng S, Zlot CH, Young SG and Rollins BJ, *et al*. MCP-1 deficiency reduces susceptibility to atherosclerosis in mice that overexpress human apolipoprotein B. J Clin Invest 1999, 103: 773–778.
5 Boring L, Gosling J, Cleary M and Charo IF. Decreased lesion formation in CCR2-/- mice reveals a role for chemokines in the initiation of atherosclerosis. Nature 1998, 394: 894–897.
6 Pasceri V, Chang J, Willerson JT and Yeh ET. Modulation of C-reactive protein-mediated monocyte chemoattractant protein-1 induction in human endothelial cells by anti-atherosclerosis drugs. Circulation 2001, 103: 2531–2534.
7 Pober JS and Sessa WC. Evolving functions of endothelial cells in inflammation. Nat Rev Immunol 2007, 7: 803–815.
8 Stoneman VE and Bennett MR. Role of apoptosis in atherosclerosis and its therapeutic implications. Clin Sci (Lond) 2004, 107: 343–354.
9 Dimmeler S, Hermann C and Zeiher AM. Apoptosis of endothelial cells. Contribution to the pathophysiology of atherosclerosis? Eur Cytokine Netw 1998, 9: 697–698.
10 Choy JC, Granville DJ, Hunt DW and McManus BM. Endothelial cell apoptosis: biochemical characteristics and potential implications for atherosclerosis. J Mol Cell Cardiol 2001, 33: 1673–1690.
11 Tricot O, Mallat Z, Heymes C, Belmin J, Leseche G and Tedgui A. Relation between endothelial cell apoptosis and blood flow direction in human atherosclerotic plaques. Circulation 2000, 101: 2450–2453.
12 Ido Y, Carling D and Ruderman N. Hyperglycemia-induced apoptosis in human umbilical vein endothelial cells: inhibition by the AMP-activated protein kinase activation. Diabetes 2002, 51: 159–167.
13 Cheng C, Tempel D, van Haperen R, van der Baan A, Grosveld F, Daemen MJ and Krams R, *et al*. Atherosclerotic lesion size and vulnerability are determined by patterns of fluid shear stress. Circulation 2006, 113: 2744–2753.
14 Bansilal S, Farkouh ME and Fuster V. Role of insulin resistance and hyperglycemia in the development of atherosclerosis. Am J Cardiol 2007, 99: 6B–14B.
15 Li QS, Liu Y, Feng ZJ, Zhang YL and Qian MZ. Monocyte chemotactic protein-1 induces the apoptosis of human umbilical vein endothelial cells. Acta Academiae Medicinae Militaris Tertiae 2007, 29: 1682–1684.
16 Li QS, Liu Y, Feng ZJ, Lu ZS and Qian MZ. The molecular mechanism of apoptosis of human umbilical vein endothelial cells induced by monocyte chemotacitic protein-1. Sheng Li Xue Bao 2010, 62: 63–68.
17 Xu Y, Liu XP, Li QS, Shang HF and Qian MZ. CCR2 mediates monocyte chemotactic protein-1 induced apoptosis in human vein endothelial cells. Chin J Biochem Mol Biol 2010, 26: 356–361.
18 Liu D, Cheng T, Guo H, Fernández JA, Griffin JH, Song X and Zlokovic BV. Tissue plasminogen activator neurovascular toxicity is controlled by activated protein C. Nat Med 2004, 10: 1379–1383.
19 Abramov AY, Smulders-Srinivasan TK, Kirby DM, Acin-Perez R, Enriquez JA, Lightowlers RN and Duchen MR, *et al*. Mechanism of neurodegeneration of neurons with mitochondrial DNA mutations. Brain 2010, 133: 797–807.
20 Morán M, Rivera H, Sánchez-Aragó M, Blázquez A, Merinero B, Ugalde C and Arenas J, *et al*. Mitochondrial bioenergetics and dynamics interplay in complex I-deficient fibroblasts. Biochim Biophys Acta 2010, 1802: 443–453.
21 Espino J, Mediero M, Lozano GM, Bejarano I, Ortiz, García JF and Pariente JA, *et al*. Reduced levels of intracellular calcium releasing in spermatozoa from asthenozoospermic patients. Reprod Biol Endocrinol 2009, 7: 11.
22 de Lemos JA, Morrow DA, Sabatine MS, Murphy SA, Gibson CM, Antman EM and McCabe CH, *et al*. Association between plasma levels of monocyte chemoattractant protein-1 and long-term clinical outcomes in patients with acute coronary syndromes. Circulation 2003, 107: 690–695.
23 Deo R, Khera A, McGuire DK, Murphy SA, Meo NJP, Morrow DA and de Lemos JA. Association among plasma levels of monocyte chemoattractant protein-1, traditional cardiovascular risk factors, and subclinical atherosclerosis. J Am Coll Cardiol 2004, 44: 1812–1818.
24 Rollins BJ, Walz A and Baggiolini M. Recombinant human MCP-1/JE induces chemotaxis, calcium flux, and the respiratory burst in human monocytes. Blood 1991, 78: 1112–1116.
25 Green DR and Reed JC. Mitochondria and apoptosis. Science 1998, 281: 1309–1312.
26 Wang X. The expanding role of mitochondria in apoptosis. Genes Dev 2001, 15: 2922–2933.
27 Marchenko ND, Zaika A and Moll UM. Death signal-induced localization of p53 protein to mitochondria. A potential role in apoptotic signaling. J Biol Chem 2000, 275: 16202–16212.
28 Schuler M and Green DR. Mechanisms of p53-dependent apoptosis. Biochem Soc Trans 2001, 29: 684–688.
29 Mihara M, Erster S, Zaika A, Petrenko O, Chittenden T, Pancoska P and Moll UM. p53 has a direct apoptogenic role at the mitochondria. Mol Cell 2003, 11: 577–590.
30 Lorenzo E, Ruiz-Ruiz C, Quesada AJ, Hernández G, Rodríguez A, López-Rivas A and Redondo JM. Doxorubicin induces apoptosis and CD95 gene expression in human primary endothelial cells through a p53-dependent mechanism. J Biol Chem 2002, 277: 10883–10892.
31 Reyland ME. Protein kinase C and apoptosis. In: Srivastava R ed. Apoptosis, Cell Signaling, and Human Diseases. Totowa, NJ: Humana Press, 2007, 31–55.
32 Khalil RA. Protein kinase C. In: Khalil RA eds. Regulation of Vascular Smooth Muscle Function. San Rafael, CA: Morgan & Claypool Life Sciences, 2010, 21–30.
33 Kock K, Koenen A, Giese B, Fraunholz M, May K, Siegmund W and Hammer E, *et al*. Rapid modulation of the organic anion transporting polypeptide 2B1 (OATP2B1, SLCO2B1) function by protein kinase C-mediated internalization. J Biol Chem 2010, 285: 11336–11347.
34 Jiang H, Cheng D, Liu W, Peng J and Feng J. Protein kinase C inhibits autophagy and phosphorylates LC3. Biochem Biophys Res Commun 2010, 395: 471–476.

35 Moench I, Prentice H, Rickaway Z and Weissbach H. Sulindac confers high level ischemic protection to the heart through late preconditioning mechanisms. Proc Natl Acad Sci USA 2009, 106: 19611–19616.
36 Hains AB, Vu MA, Maciejewski PK, van Dyck CH, Gottron M and Arnsten AF. Inhibition of protein kinase C signaling protects prefrontal cortex dendritic spines and cognition from the effects of chronic stress. Proc Natl Acad Sci USA 2009, 106: 17957–17962.
37 Rafiee P, Nelson VM, Manley S, Wellner M, Floer M, Binion DG and Shaker R. Effect of curcumin on acidic pH-induced expression of IL-6 and IL-8 in human esophageal epithelial cells (HET-1A): role of PKC, MAPKs, and NF-kappaB. Am J Physiol Gastrointest Liver Physiol 2009, 296: G388–398.
38 Herbert JM, Augereau JM, Gleye J and Maffrand JP. Chelerythrine is a potent and specific inhibitor of protein kinase C. Biochem Biophys Res Commun 1990, 172: 993–999.
39 Niu J, Azfer A, Zhelyabovska O, Fatma S and Kolattukudy PE. Monocyte chemotactic protein (MCP)-1 promotes angiogenesis via a novel transcription factor, MCP-1-induced protein (MCPIP). J Biol Chem 2008, 283: 14542–14551.
40 Charo IF. Monocyte-endothelial cell interactions. Curr Opin Lipidol 1992, 3: 335–343.
41 Hesselgesser J, Taub D, Baskar P, Greenberg M, Hoxie J, Kolson D and Horuk R. Neuronal apoptosis induced by HIV-1 gp120 and the chemokine SDF-1 alpha is mediated by the chemokine receptor CXCR4. Curr Biol 1998, 8: 595–598.
42 Herbein G, Mahlknecht U, Batliwalla F, Gregersen P, Pappas T, Butler J and O'Brien W, *et al*. Apoptosis of CD8+ T cells is mediated by macrophages through interaction of HIV gp120 with chemokine receptor CXCR4. Nature 1998, 395: 189–194.
43 Mellado M, de Ana A, Moreno M, Martínez C and Rodríguez-Frade JM. A potential immune escape mechanism by melanoma cells through the activation of chemokine-induced T cell death. Curr Biol 2001, 11: 691–696.
44 Glaser J, Gonzalez R, Sadr E and Keirstead HS. Neutralization of the chemokine CXCL10 reduces apoptosis and increases axon sprouting after spinal cord injury. J Neurosci Res 2006, 84: 724–734.
45 Dimmeler S and Zeiher AM. Endothelial cell apoptosis in angiogenesis and vessel regression. Circ Res 2000, 87: 434–439.
46 Brooks PC, Montgomery AM, Rosenfeld M, Reisfeld RA, Hu T, Klier G and Cheresh DA. Integrin alpha v beta 3 antagonists promote tumor regression by inducing apoptosis of angiogenic blood vessels. Cell 1994, 79: 1157–1164.
47 Papapetropoulos A, Fulton D, Mahboubi K, Kalb RG, O'Connor DS, Li F and Altieri DC, *et al*. Angiopoietin-1 inhibits endothelial cell apoptosis via the Akt/survivin pathway. J Biol Chem 2000, 275: 9102–9105.
48 Hong KH, Ryu J and Han KH. Monocyte chemoattractant protein-1-induced angiogenesis is mediated by vascular endothelial growth factor-A. Blood 2005, 105: 1405–1407.
49 Salcedo R, Ponce ML, Young HA, Wasserman K, Ward JM, Kleinman HK and Oppenheim JJ, *et al*. Human endothelial cells express CCR2 and respond to MCP-1: direct role of MCP-1 in angiogenesis and tumor progression. Blood 2000, 96: 34–40.
50 Zhou L, Azfer A, Niu J, Graham S, Choudhury M, Adamski FM and Younce C, *et al*. Monocyte chemoattractant protein-1 induces a novel transcription factor that causes cardiac myocyte apoptosis and ventricular dysfunction. Circ Res 2006, 98: 1177–1185.